2.2 DUAL-DOPPLER LIDAR OBSERVATIONS OVER WASHINGTON DC

Rob Newsom*[,1], David Ligon[2], Dennis Garvey[2]

[1]Pacific Northwest National Laboratory, Richland, WA

[2]Army Research Laboratory, Adelphi, MD

1. INTRODUCTION

In May 2004 a field campaign was conducted to study transport and diffusion over the central Washington DC area (Warner et al 2007). A number of in-situ and remote sensing meteorological instruments were deployed to measure atmospheric stability and wind flow patterns ranging from building- to urban-scale. This study uses observations made by two coherent Doppler lidars in order to investigate the detailed flow structure over the central Washington DC area. Estimates of boundary layer height derived from lidar backscatter data and from radiosonde temperature soundings are compared. We also compare estimates of mean wind profiles derived from VAD analyses of each of the lidars.

Figure 1 shows the locations of the two lidars, and the location of a radiosonde release site (DPG RAOB). The first lidar was deployed atop the Navy Annex building, immediately south of Arlington National Cemetery. A second lidar, operated by the Army Research Laboratory, was deployed approximately 5 km to the southeast of the Annex lidar, next to the Potomac River at Bolling Air Force Base.

During the two week deployment both lidars performed overlapping volume scans and were operated more or less continuously. The region of overlap between the two volume scans includes the Potomac River, East Potomac Park, the National Mall, and tidal basin areas. Table 1 lists the times of the five intensive observation periods (IOPs) that were conducted during the course of the two week field experiment.

2. SCAN STRATEGIES

Both the Annex and Bolling systems are eye-safe WindTracer lidars manufactured by Lockheed Martin Coherent Technologies (Henderson et al. 1991, 1993). These instruments employ solid state laser transmitters operating at a wavelength of 2μm, with a 400 ns (60 m) 2 mJ pulse, at a pulse repetition frequency (PRF) of 500 Hz. The range gate size for both lidars was 72 m during the field experiment.

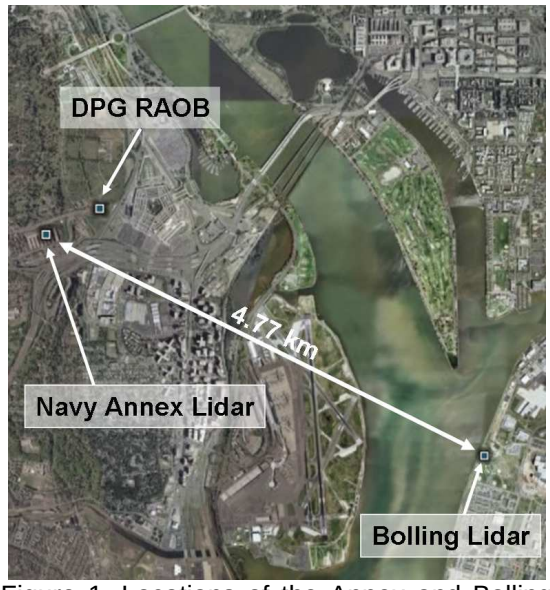

Figure 1. Locations of the Annex and Bolling lidars during the field experiment. Also shown is the location of radiosonde release site (DPG RAOB). The Potomac River is clearly visible, and the National Mall area is in the northeast corner.

IOP	Start	End
1	22:30 04 May	07:15 05 May
2	22:30 06 May	07:15 07 May
3	23:30 08 May	05:15 09 May
4	22:15 10 May	04:30 11 May
5	22:20 12 May	04:15 13 May

Table 1. IOP times as defined by the availability of radiosonde data from the DPG RAOB site.

Both lidars maintained essentially the same scan strategies throughout the duration of the field project. The Bolling lidar performed

* *Corresponding author address*: Rob K. Newsom, Pacific Northwest National Laboratory, P.O. Box 999, MSIN K9-30, Richland, WA 99352; e-mail: rob.newsom@pnl.gov

volume scans over the northwest sector (between 270° and 360° azimuth) using 10 elevation angles ranging from 0.9 to 9. The Annex lidar performed volume scans toward the east-northeast (between 32° and 122° azimuth), with 10 elevation angles ranging from -1.0 to 21.5. Thus, the volume scans performed by the Bolling lidar were shallower with finer elevation resolution than the volume scans performed by the Annex lidar. At the conclusion of each volume scan, both lidars executed a complete 360° VAD scan at an elevation angle of 24°. The time to complete a single volume and VAD scan was approximately 5 minutes for both systems.

3. LIDAR DATA QUALITY

The Annex lidar performed exceptionally well during the deployment; however, the Bolling lidar experienced some problems due to a malfunction of its transceiver. During the daytime the Bolling lidar tended to perform well, but its performance would gradually deteriorate at night. Inspection of the pulse monitor (PM) signal from the Bolling lidar indicated that the pulse energy often fell well below its optimal operating range during the night. The reason for this behavior was later determined to be caused by drift in a phased-lock loop controlling the offset frequency in the transceiver.

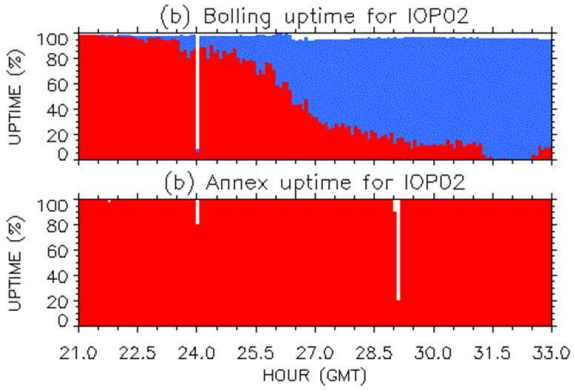

Figure 2. Time series of data availability for (a) the Bolling and (b) the Annex lidars during IOP 2. Blue indicates periods when the lidar was operating, while the red indicates the fraction of time that the pulse monitor signal was above a prescribed minimum level.

Data quality control was performed by rejecting radial velocity profiles corresponding to abnormally low PM values. This quality control procedure was effective at rejecting poor quality radial velocity measurements. Unfortunately, this resulted in the rejection of a large fraction of the nighttime data from the Bolling lidar. Figure 2 presents time series of the availability of data from the Annex and Bolling lidars during IOP 2. The blue areas in this figure indicate the fraction of time that the systems were operating, and the red areas indicate the fraction of time that the systems operated above a prescribed lower PM threshold value. As indicated in Figure 1, the Annex lidar tended to perform quite well overall, while the Bolling lidar did well during the day, but then experienced a gradual deterioration at night.

4. VAD ANAYLSIS

A modified VAD analysis (Banta et al. 2002) was conducted separately using the Annex and Bolling radial velocity measurements. The VAD results for all 5 IOPs are shown in Figures 3 through 7. These plots show the mean wind speed and wind direction as a function of normalized height and time in hours after 00 UTC on the start day of the IOP. We note that for this location and this time of the year, sunrise occurs at about 10 UTC, and sunset occurs at about 00 UTC. Thus, the nighttime period extends from hours 24 through 34 in these plots.

Figures 3 through 7 all show the formation, growth and subsequent dissipation of a low-level jet (LLJ) structure. For all IOPs the winds were southerly near the surface and then veered toward westerly with height. The maximum in the LLJ occurred at roughly the same height during all 5 IOPs with the exception of IOP 3, in which the maximum was slightly higher. The LLJ tended to form a couple hours after sunset and reach its maximum strength between 03 and 07 UTC,

Figure 3 through 7 also show good agreement between the Annex and Bolling lidars. The VAD results for the Bolling lidar were remarkably good despite the problems with its transmit laser during the nighttime periods. The reason for this is that there was always at least a small fraction of profiles for which the PM signal exceeded the threshold value used in the QC algorithm. With a suitable choice of averaging time the VAD algorithm is able to construct very reasonable wind profiles using intermittent observations. In this case, the averaging time was 30 minutes.

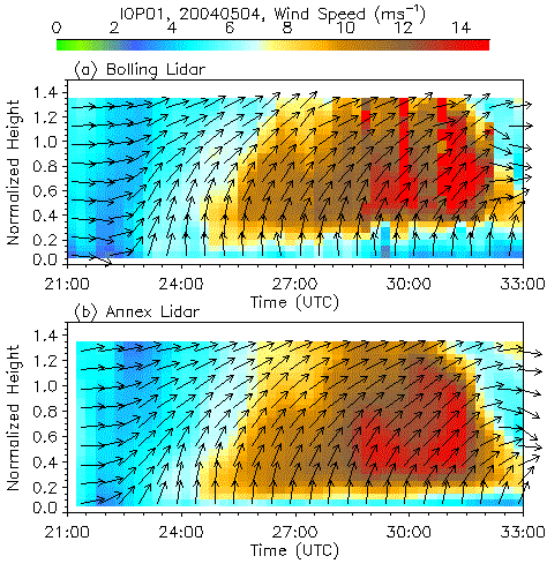

Figure 3. Mean winds derived from the (a) Bolling and (b) Annex lidars for IOP 1. Colors indicate wind speed and arrows indicate wind direction (the arrows point in the direction of the flow).

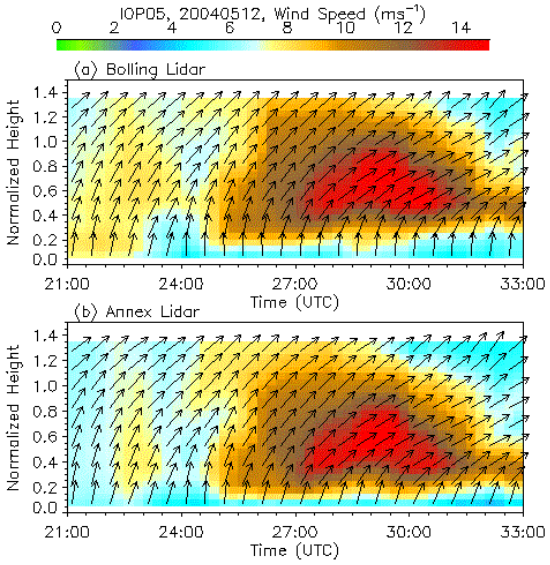

Figure 4. Same as Fig 3 except for IOP 2.

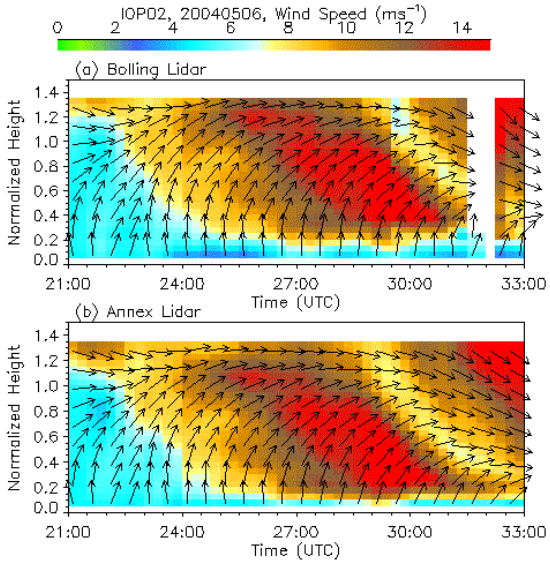

Figure 5. Same as Fig 3 except for IOP 3.

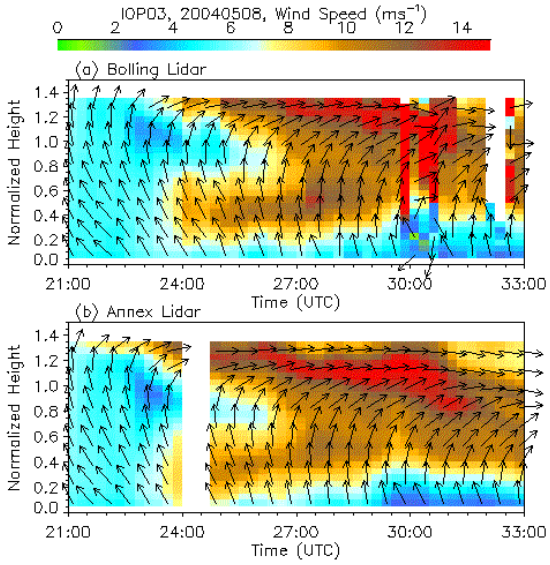

Figure 6. Same as Fig 3 except for IOP 4.

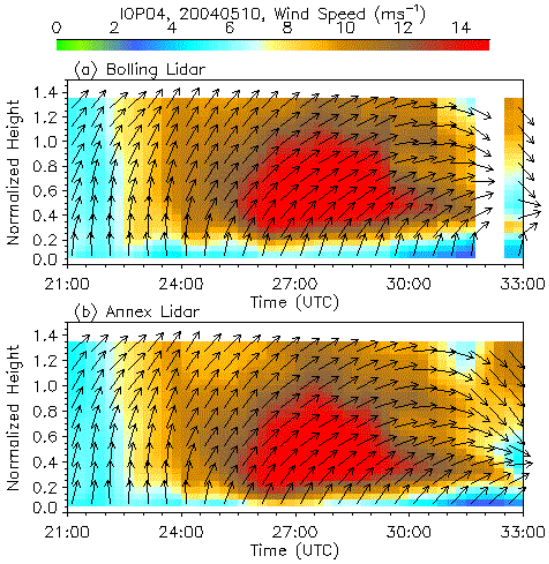

Figure 7. Same as Fig 3 except for IOP 5.

5. BOUNDARY LAYER HEIGHT

This section investigates the relationships between the signal strength measured by the lidar and the potential temperature structure measured by the radiosonde. Figures 8 through 12 show comparisons between the vertical gradient of the Annex lidar signal-to-noise-ratio (SNR), and potential temperature soundings from the DPG radiosondes. Time-height cross sections of SNR were obtained by averaging profiles from individual VAD scans and converting range along the beam to height above ground.

It is important to note that the SNR as displayed in Figures 8 through 12 is in dB and has not been corrected for $1/r^2$ attenuation. As a result, the vertical gradient of this field exhibits a constant value in layers where the backscatter and extinction due to aerosol is constant with height. Sharp negative (positive) gradients generally indicate a decrease (increase) in the aerosol backscatter with height.

Figures 8 through 12 clearly show the correlations between the vertical gradient of the SNR field and the stratification in potential temperature. We note that under convective daytime conditions the maximum negative gradient in SNR typically occurs just below the base of the capping inversion layer. Also, IOP 3 is particularly interesting because the aerosol backscatter exhibits a very distinctive stratification at low levels.

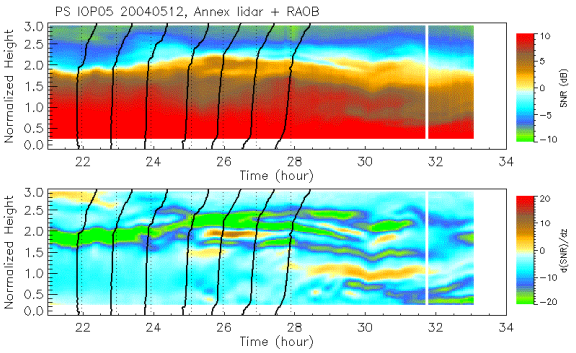

Figure 8. Time-height cross sections of SNR (top) and the vertical derivative of SNR (bottom) for IOP 1. Solid black lines represent profiles of potential temperature, with the sounding times indicated by the vertical dotted lines. The SNR data was measured by the Annex lidar.

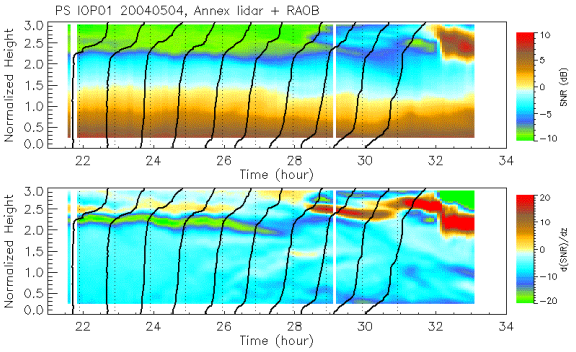

Figure 9. Same as Figure 8, except for IOP 2.

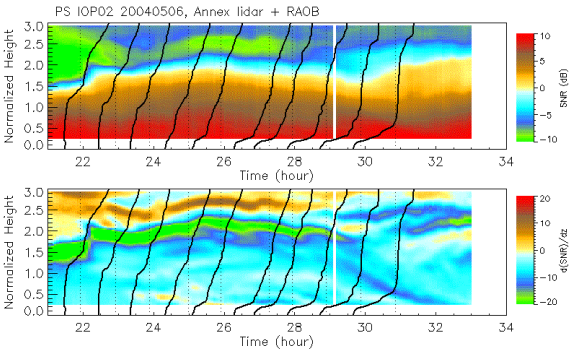

Figure 10. Same as Figure 8, except for IOP 3.

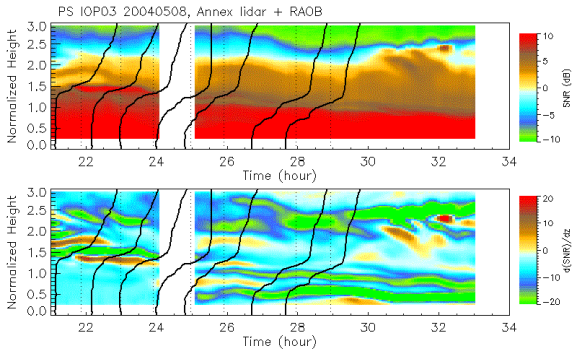

Figure 11. Same as Figure 8, except for IOP 4.

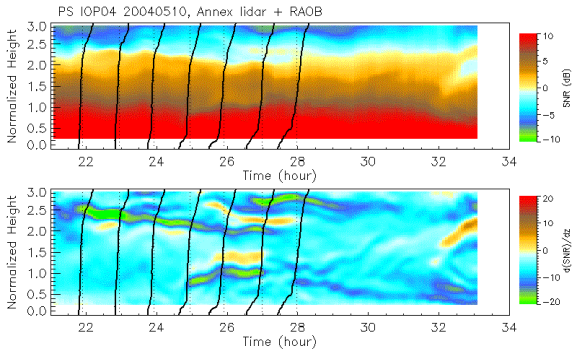

Figure 12. Same as Figure 8, except for IOP 5.

6. DUAL-DOPPLER RETRIEVALS

Radial velocity data from the Annex and Bolling lidars were combined in a dual-Doppler analysis to retrieve low altitude horizontal vector wind fields. The method of analysis is described by Newsom, et al. (2007).

Figure 13 displays examples of dual-Doppler retrievals during IOP 1 on 4-5 May 2004. The Annex lidar was used as the reference; thus, the UTM coordinate system shown in Figure 13 has been shifted such that the Annex lidar defines the origin. Scan data from the lowest (positive) elevation angle (1.5^o) of the Annex lidar was combined with the lowest three elevation angle scans from the Bolling lidar (0.9^o, 1.8^o, and 2.7^o). Distortions induced by non-simultaneous measurements were minimized by using only those observations that occur within a 1 minute time window centered on the mean time of the Annex scan, and within a prescribed height layer.

All days for which there were dual Doppler measurements available were analyzed in the manner described above. A total of 917 individual retrievals were obtained spanning the period from 19:03 UTC on 1 May to 13:10 UTC on 13 May, 2004. The quality of these retrievals vary considerably. Daytime and early nighttime periods generally resulted in better quality and higher density retrievals, while early morning periods were more problematic due to the malfunctions experienced by the Bolling lidar during these periods.

6. SUMMARY

This paper presented preliminary results from the analysis of Doppler lidar data acquired during the May 2004 field campaign in Washington DC. This included comparisons between VAD results derived from the Annex and Bolling lidars, comparisons between lidar backscatter measurements and potential temperature soundings, and the results of dual-Doppler analysis to derived the detailed flow structure over the central Washington DC area.

Acknowledgements. Funding for this work was provided by DTRA through the Army Research Office. We thank Dr. Walter Bach at the Army Research Office.

References

Banta R.M., R.K. Newsom, J. K. Lundquist, Y. L. Pichugina, R. L. Coulter, and L. D. Mahrt, 2002: Nocturnal low-level jet characteristics over Kansas during CASES-99. *Boundary-Layer Meteor*, **105**, 221-252.

Henderson, S. W., C. P. Hale, J. R. Magee, M. J. Kavaya, A. V. Huffaker, 1991: Eye-safe coherent laser radar system at 2.1 μm using TmHo:YAG lasers. *Opt. Lett.*, **16**, 773-775.

_____, P. J. M. Sunni, C. P. Hale, S. M. Hannon, J. R. Magee, D. L. Bruns, E. H. Yuen, 1993: Coherent laser radar at 2 μm using solid-state lasers. *IEEE Trans. Geo. Remote Sensing*, **31**, 4-15.

Newsom R. K., R. Calhoun, D. Ligon, J. Allwine. 2008: Linearly Organized Turbulence Structures Observed over a Suburban Area by Dual-Doppler Lidar. *Boundary-Layer Meteor,* **127**, 111-130.

Warner T., et al., 2007: The Pentagon Shield Field Program, toward critical infrastructure protection. Bull. Amer. Meteorol. Soc., **88**, 167-176.

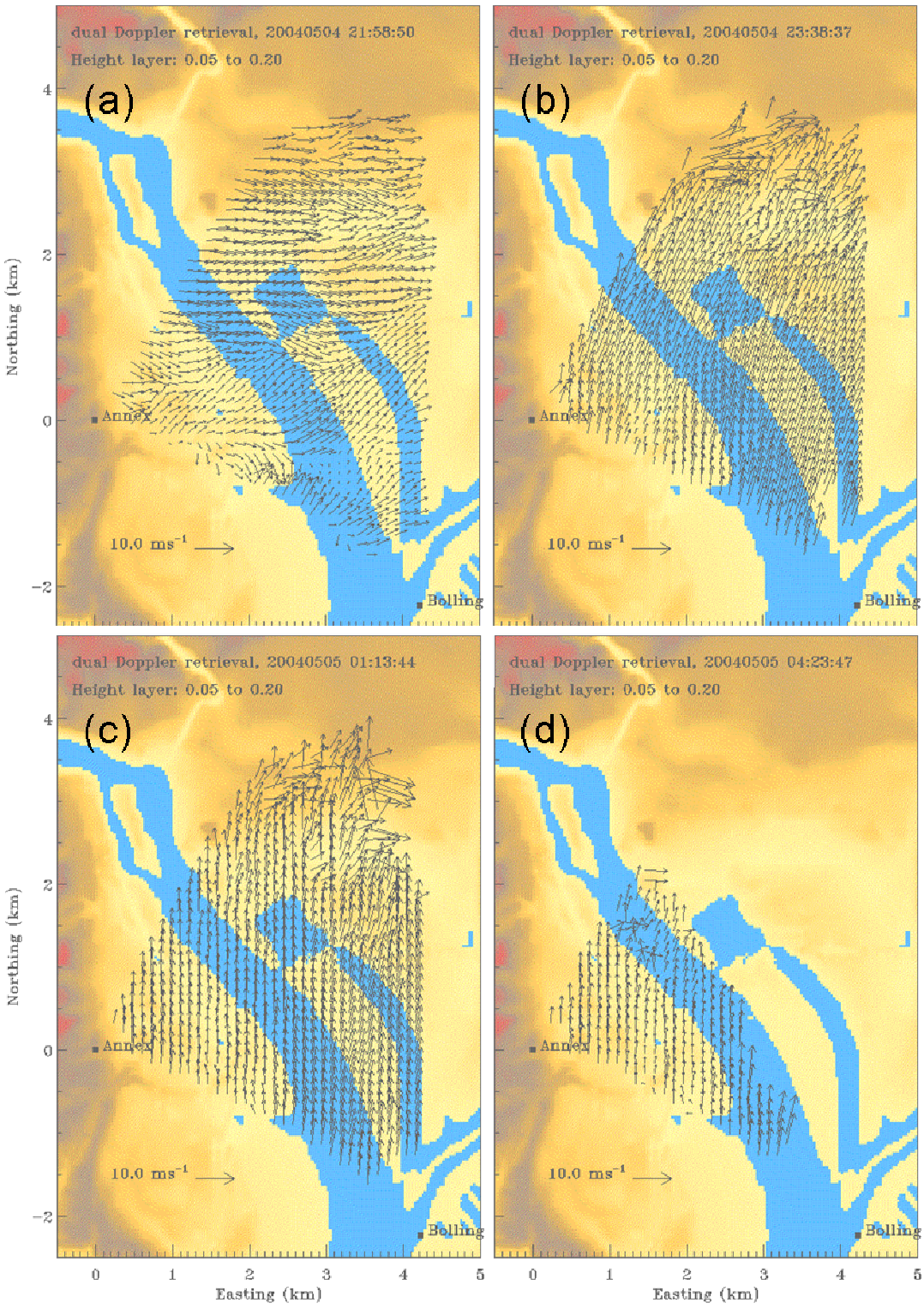

Figure 13. Horizontal wind velocity vector fields obtained from dual Doppler analysis of the Annex and Bolling lidars during IOP 1 at (a) ~22:00 UTC on 4 May 2004, (b) ~22:40 UTC on 4 May 2004, (c) ~01:10 UTC on 5 May 2004, and (d) ~04:20 UTC on 5 May 2004.